Gait & Posture 69 (2019) 169–175

Contents lists available at ScienceDirect

Gait & Posture

journal homepage: www.elsevier.com/locate/gaitpost

Full length article

Recurrence dynamics reveals differential control strategies to maintain balance on sloped surfaces

Aviroop Dutt-Mazumder[a,*], Adam C. King[b], Karl. M. Newell[c]

[a] Department of Physical Medicine & Rehabilitation, University of Michigan, United States
[b] Department of Kinesiology, Texas Christian University, United States
[c] Department of Kinesiology, University of Georgia, United States

ARTICLE INFO

Keywords:
Postural control
Virtual time-to-contact
Sloped surfaces
Recurrence dynamics
Upright standing
Balance

ABSTRACT

Background: Studies on postural control have primarily focused on the maintenance of balance in quiet upright standing on flat horizontal support surfaces that can reveal only a subset of the potential postural stability/instability configurations in everyday contexts.
Objectives: Here we investigated the nature of dynamical properties of postural coordination in an upright standing task as a function of the systematic scaling of seven support surface angles, +20°, +10° dorsiflexion (+), 0 °Flat, −10°, −20°, −30°, −35° plantarflexion (−), mounted on a force plate.
Methods: The center of pressure (CoP) and virtual time-to-contact (VTC) were analyzed to examine the spatial and spatio-temporal aspects of postural coordination dynamics, respectively. Recurrence quantification analysis (RQA) was used to characterize the dynamic postural control strategies as a function of slope surface angle.
Results: The recurrence findings showed that on a flat surface the postural CoP dynamic are recurrent with a largely deterministic process and higher Shannon entropy compared to elevated slope angles in dorsiflexion and plantarflexion. There were asymmetrical patterns between similar slope angles for dorsiflexion and plantarflexion postures. The recurrence measures revealed that VTC operates on a higher embedding dimension than that of CoP.
Significance: VTC showed an enhanced sensitivity to detection of postural instability in relation to the stability boundary that was magnified on the flat surface but progressively reduced over larger surface angles for both the dorsiflexion and plantarflexion postures.

1. Introduction

Maintenance of postural control in quiet standing is a complex task that requires the integration of sensory-motor processes that collectively organize to maintain postural stability [1,2]. Previous investigations on postural control have predominantly manipulated postural difficulty through changes in postural configuration [2] and foot orientation [3] to examine the control processes. To further challenge postural stability, sloped support surfaces [4] can be used to understand how the vertical projection of the center of mass and center of pressure (CoP) are preserved within the base of support [5]. Here, we examine how different sloped surfaces influence the continuous, low-amplitude but complex motion of the CoP during upright stance. The collective organization of CoP has been shown to be a reflection of the synergies encompassing joint coordination, sensorimotor processes and adaptions to ongoing internal and external perturbations [2].

Typically during quiet standing, CoP exhibits non-stationary fluctuations [6], and as a means to supplement traditional CoP spatial metrics (e.g., CoP area, displacement and its derivatives), frequency and non-linear analyses have been employed to investigate the time-dependent CoP structures [7]. Moreover, analysis tools that can delineate the underlying linear and non-linear dynamics have revealed a blend of deterministic and stochastic processes in postural control [8]. Indeed, the dynamic fluctuations of CoP trajectories do not reflect the properties of random noise but rather contain temporal structures indicative to persistent and flexible postural control strategies [9].

Detrended fluctuation analysis [10] and RQA [11] have shown that the nature of CoP fluctuations operates over an adaptable range of behavioral dynamics in a number of actions (e.g., gait stride intervals, finger tapping) and are governed by experimental constraints [3,12]. In

* Corresponding author at: Department of Physical Medicine & Rehabilitation, University of Michigan, 325 E Eisenhower Parkway, Suite 3013, Ann Arbor, MI, 48108, United States.
E-mail address: daviroop@umich.edu (A. Dutt-Mazumder).

https://doi.org/10.1016/j.gaitpost.2019.01.040
Received 2 August 2018; Received in revised form 28 January 2019; Accepted 29 January 2019

particular, RQA reveals the dynamics of a higher-dimensional signal depiction (i.e., phase-space reconstruction) to quantify several properties within the signal [13,14]. Specifically, the regularity and laminarity of the reconstructed signal have been associated with the concepts of flexible and rigid postural control strategies [12,15,16].

A complementary approach to understanding the mechanism of postural control has been through the spatio-temporal CoP structures of virtual time-to-contact (VTC) [17]. VTC extracts the instantaneous CoP vectors, then projected towards the enclosed postural stability boundary to calculate the estimated time it would take the CoP vectors to reach the stability boundary should the motion of CoP continue with the initial condition dynamics. A more stable postural control configuration would have more time to reach the stability boundary, whereas an unstable posture would have reduced VTC values [18,19] and hence limited temporal margins of stability.

This study examines the contrasting recurrent dynamics of the CoP and VTC timeseries as a function of the task constraints of maintaining upright postural stability across different sloped support angles. It was hypothesized that deviation from the flat support surface will result in more stable and regular dynamics of CoP and VTC trajectories that will be reflected in the differential properties of recurrence dynamics. Furthermore, we anticipated that the analysis of CoP and VTC would reveal different embedding dimensions in the reconstructed state space, that reflects their spatial and spatio-temporal postural control timescale profiles, respectively.

2. Materials and methods

2.1. Participants

Sixteen healthy participants (height range: 163–182 cm, age range: from 23 to 37 years old, and body-mass range: 55–89 kg), provided written informed consent for their participation and were recruited according to an experimental protocol approved by the Institutional Review Board. All participants were healthy and self-reported no apparent neurological disorders and musculoskeletal injuries that could influence postural control.

2.2. Instrumentation

An AMTI force platform (OPT400600-1000, Watertown, MA) was used to derive the displacement of the CoP. Pre-fabricated wooden platform wedges of different angles, +20˚, +10˚ dorsiflexion (+), 0 ˚Flat, -10˚, -20˚, -30˚, -35˚ plantarflexion (-) were mounted on the force platform to provide slope surfaces. The slope angles were based on pilot tests of the biomechanical limits of ankle angle range of motion for the population group. The platform wedge surfaces were covered with commercial sand paper of grain size 100 to standardize the coefficient of friction across all platform wedge angle conditions. The data were sampled at 100 Hz and were digitally low-pass filtered with a second order Butterworth filter with a cut-off frequency of 5 Hz based on previous techniques to reveal inherent physiological information [20].

2.3. Experimental procedures

Participants were instructed to maintain upright postural balance while standing on the force platform with bare feet, eyes open. They focused on a visual target placed 2 m away from the platform at eye level and maintained foot placement on the wedge for 40 s. The order of the platform angles was assigned randomly, with the baseline (0˚ horizontal) as the first trial. Each platform condition had 2 trials with 2 min. rest between each trial. There was 4 min. of recovery time between each platform condition. For each platform condition a supplementary trial was used to evaluate the functional stability boundary, where the participant was asked to lean as far as they could in 8 equally spaced directions within an ellipse surrounding the center of the base of support while maintaining the same foot placement throughout the entire trial [4].

2.4. Calculation of CoP and VTC

CoP was analyzed from the force plate along both x (ML: mediolateral) and y (AP: anterior-posterior) directions on which the platform wedges were mounted [5]. CoP area represents the area enclosed with the CoP trajectories with 95% confidence interval, CoP length is the total length of the CoP sway for the trial duration, and the functional stability boundary area is that area enclosed within the CoP while doing maximum excursion. postures across 7 directions. VTC was computed as in Slobounov et al. [17] and provides a direct measure of the relation of the CoP kinematics to the functional stability boundary. The VTC (τ) at each time (40 s at 100 Hz) was computed (**Appendix A**). All analyses were performed in custom written scripts with MATLAB (2017b).

2.5. Calculation of recurrence measures

In the recurrence plots, data points form darkened *diagonal lines* and the organization of these data points is used to quantify the structural properties of the reconstructed signal (**Appendix B** & Fig. 1). The spatial organization reflects several dynamic properties of the signal and the current investigation focused on: *%REC* (percent recurrence), *ENT* (Shannon entropy), *%DET* (percent determinism), and *%LAM* (percent laminarity) [13].

%REC is the amount of recurring points, expressed as a percentage of the number of possible recurring points. It is a measure of the relative density of recurrence points in the sparse matrix and is related to the definition of the correlation sum:

$$\%REC = \frac{1}{N^2 - N}\sum_{i \neq j}^{N} R_{i,j} \tag{1}$$

where R is the Euclidian radius that was used as a measure to calculate the tolerance in the state space, and N is the number of considered states. We predicted that during quiet standing on a flat surface, the *%REC* would be significantly higher than other ankle angle conditions [21].

The *%DET* is defined as the fraction of recurrence points that forms *diagonal lines* and reflects the probability that states will occur (Eq 2). Systems possessing deterministic dynamics are characterized by the *diagonal lines* and can be interpreted as the predictability of the system more so for periodic behaviors than chaotic process.

$$\%DET = \sum_{l=d_{min}}^{N} l\, H_D(l) / \sum_{i,j=1}^{N} R_{i,j} \tag{2}$$

We predicted that the CoP and VTC signals would be highly stationary with longer quasi-periodic balance strategies at the flat surfaces and lower slope angles as reflected by higher *%DET*.

The *ENT* measure is computed with respect to the deterministic structure of the recurrence plot and reflects the complexity of the deterministic structure (Eq 3). Entropy should be highest for flat support surfaces when compared to sloped surfaces [4].

$$ENT = -\sum_{l=d_{min}}^{N} p(l) \ln p(l) \tag{3}$$

where $p(l) = H_D(l) / \sum_{l=d_{min}}^{N} H_D(l))$, and $H_D(l)$ is the histogram of the *diagonal lines*.

%LAM was defined as the relative amount of vertical structuring over the entire recurrence map that is analogous to *%DET* for recurrence points in *diagonal lines*. The *vertical lin*e structures are used to compute the %*LAM* and mark time intervals in which the system does not change or changes very slowly. For postural control, a CoP signal that consists of longer, more rigid states may be less flexible in

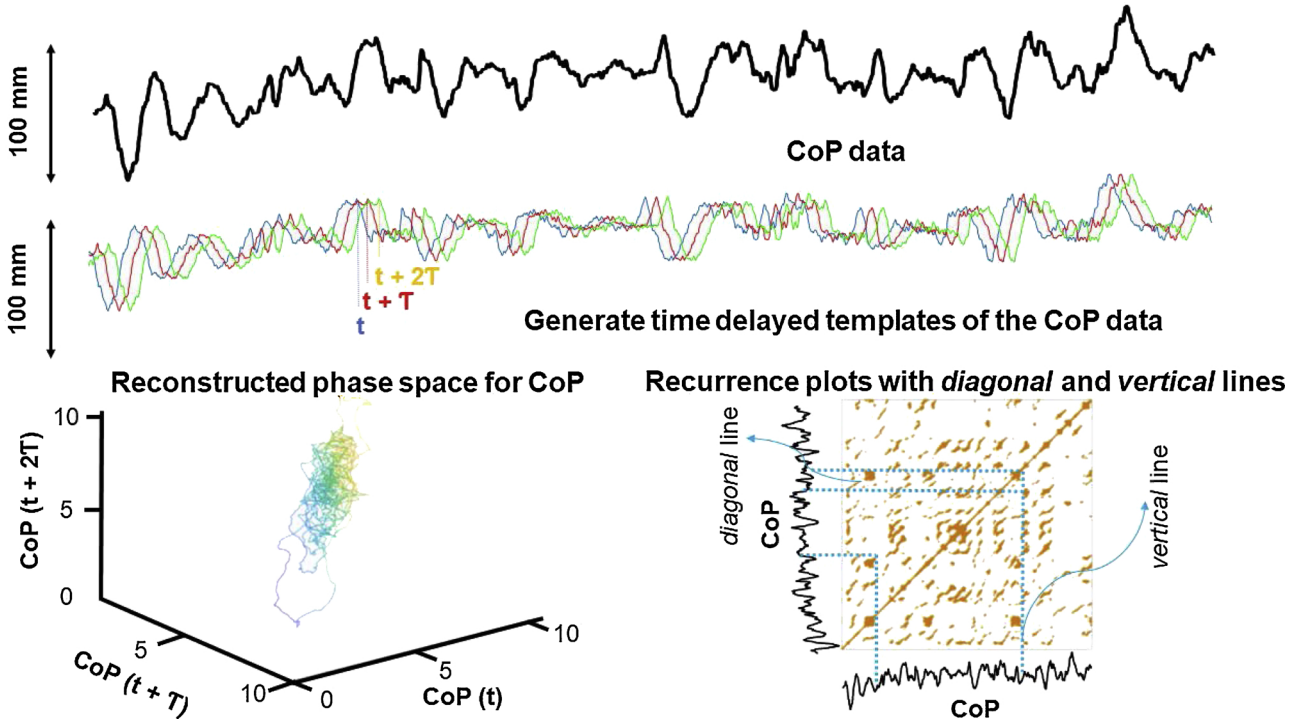

Fig. 1. Representative recurrence plots of CoP motion. Example of CoP (blue), time delay of 10 ms (red), and time delay of 20 ms (green). Thereafter, phase space was reconstructed by plotting the time-delayed templates across the three axes. Note it is a 3D plot, but analysis was done for 5D in CoP, and 8D for VTC. Finally, the recurrence plot represents the recurrence dynamics in the reconstructed phase space. See Appendix B for detailed methods (For interpretation of the references to colour in this figure legend, the reader is referred to the web version of this article).

maintaining its trajectory within the base of support when faced with sloped surfaces.

2.6. Statistics

A two-way repeated measures ANOVA (7 slopes x 2 trials) was employed on the CoP and VTC standard discrete variables to study the main effect differences of slopes, trials and the interaction effect between slopes and trials. A 2nd order polynomial was fit to predict the overall trend line for each RQA variable to test for the effect of slope for each trial, where p_1, p_2, p_3 are the co-efficients with 95% confidence interval (Eq. (4)).

$$f(x) = p_1 * x^2 + p_2 * x + p_3 \quad (4)$$

We evaluated the general linearity and homogeneity of variances to test statistical assumptions. The dependent variables were computed from CoP (AP and ML) motion as well as the VTC trajectories. Standard goodness of fit output consisting of root mean square error (RMSE), and adjusted R^2 were reported for each dependent variable on each trial. Significance was assumed when there was less than 5% chance for Type I error. When appropriate, Tukey's post hoc analysis was performed to test for significance between the sloped surface conditions. For clarity purposes only, single trial graphs were illustrated for the recurrence measures.

3. Results

3.1. CoP and VTC across platform slope conditions

The main effect of platform condition was significant for CoP area, $F(6224) = 13.88$ ($p < 0.001$), CoP length, $F(6224) = 75.53$ ($p < 0.001$), functional stability area, $F(6224) = 142.85$ ($p < 0.001$), and VTC, $F(6224) = 125.91$ ($p < 0.001$). Post-hoc Tukey analysis showed that CoP area and length on the flat condition were significantly lower than other slope angles, and the stability boundary area and VTC on flat were significantly higher than other slope angles (Table 1). The main effects for trials and the interaction between slope conditions and trials were nonsignificant ($p > 0.15$).

3.2. Recurrent dynamics parameters for CoP and VTC

Our custom written automated algorithm was designed to fit a nth order regression that would minimize the cost-function (root mean square error and adjusted R^2). The resultant output showed that a 2nd order polynomial regression provided the highest goodness of fit. Table 2 provides for each trial the 2nd order polynomial regression equation along with their standard goodness of fit for each recurrent dynamics' parameter (*%REC, %DET, ENT*, and *%LAM*) for CoP (ML and AP) and VTC values as a function of platform slope conditions.

Fig. 2**a** shows the mean *%REC* for CoP-ML, CoP-AP, and Fig. 2**b** the VTC together with their corresponding 2nd order polynomial fit for each dependent variable as a function of slope condition for a representative trial. Similarly, Fig. 3**a** shows the mean *%DET* for CoP-ML, CoP-AP, and Fig. 3**b** the VTC and their corresponding 2nd order polynomial fit. Fig. 4**a** shows the mean *%LAM* for CoP-ML, CoP-AP, and Fig. 4**b** the VTC and their corresponding 2nd order polynomial fit.

In general, CoP-ML had a higher adjusted R^2 values (0.95 - 0.81) than CoP-AP (0.93 - 0.51) for *%REC* parameter. The RQA findings can be summarized as follows: a) on a flat surface the postural CoP dynamics is recurrent with a largely deterministic process and higher Shannon entropy compared to elevated slope angles in dorsiflexion and plantarflexion; b) there were asymmetrical patterns between similar slope angles for dorsiflexion and plantarflexion postures; and c) the recurrence measures revealed that VTC operates on a higher embedding dimension than that of CoP consistent with its enhanced sensitivity to detection of postural instability in relation to the stability boundary.

Table 1
CoP and VTC mean and standard deviation values across sloped platform conditions for trial 1 and trial 2 separately.

Slope Angle	−35°		−30°		−20°		−10°		0°		+ 10°		+ 20°	
Ankle Angle	Plantarflexion								Neutral		Dorsiflexion			
Trial Number	1	2	1	2	1	2	1	2	1	2	1	2	1	2
CoP area (cm^2)	2.9 ± 0.5	2.6 ± 0.5	2.5 ± 0.5	2.2 ± 0.5	1.7 ± 0.4	1.5 ± 0.3	0.9 ± 0.2	0.7 ± 0.1	0.7 ± 0.1	0.6 ± 0.1	1.2 ± 0.2	1.3 ± 0.2	3.7 ± 0.6	2.7 ± 0.5
CoP length (cm)	132.5 ± 9.0	129.4 ± 9.1	105.9 ± 8.2	101.1 ± 7.7	66.6 ± 3.8	65.9 ± 4.8	41.4 ± 2.2	39.5 ± 1.8	31.9 ± 1.7	30.3 ± 1.7	45.8 ± 2.9	41.6 ± 2.1	90.6 ± 9.6	74.5 ± 7.3
Functional stability area (cm^2)	32.4 ± 2.8	32.4 ± 2.6	46.0 ± 3.1	46.0 ± 3.2	65.1 ± 4.7	65.1 ± 4.6	77.3 ± 4.3	77.3 ± 4.5	79.1 ± 3.6	79.1 ± 4.0	76.6 ± 4.2	76.6 ± 4.4	51.3 ± 3.6	53.3 ± 4.3
VTC (s)	0.3 ± 0.0	0.3 ± 0.0	0.4 ± 0.0	0.4 ± 0.0	0.5 ± 0.0	0.5 ± 0.0	0.6 ± 0.0	0.6 ± 0.0	0.7 ± 0.0	0.7 ± 0.0	0.6 ± 0.0	0.6 ± 0.0	0.4 ± 0.0	0.4 ± 0.0

4. Discussion

This study used recurrence quantification analysis on the postural metrics of CoP and VTC trajectories to investigate their underlying control dynamics as a function of slope of the surface providing postural support. The attractor dynamic properties of recurrence (*%REC*), regularity (*%DET*), complexity (*ENT*) and laminarity (*%LAM*) of the CoP-ML, CoP-AP and VTC trajectories showed differential scaling of postural control strategies as a function of slope for upright quiet standing. The findings clearly showed that upright postural control strategies on sloped surfaces are adapted qualitatively from those of quiet standing on flat horizontal surfaces – postural organization was a product of slope inducing enhanced dispersion of CoP motion and reduced area of the stability region [19,27].

An inverted-U shaped trend over slope angles was found for all recurrence measures with deviations from the flat support surface condition altering both the CoP and VTC dynamics. Consistent with previous studies, directional changes of CoP dynamics were associated with specific task constraints. For example, King et al. [3] found that the directional change of CoP regularity and complexity depended on the AP and ML stability, particularly in the most challenging postural stances (e.g., staggered and tandem). Here, the similar polynomial fits for CoP-ML, CoP-AP revealed that sloped surfaces altered AP and ML stability in a comparable manner, which is consistent with previous evidence regarding the regulation of postural control under manipulations of visual information structure [21], and altered sensory input [15].

The recurrent properties of both CoP trajectories differed consistently across the sloped conditions, more prominently at the most elevated dorsiflexion angles. This trend was present across all recurrence measures. For both CoP trajectories and VTC, the flat support surface yielded the most recurrent, deterministic, and complex trajectories while the inclined and declined angles resulted in more stochastic but less complex signals. The obtained inverted-U shaped function for the deterministic and complexity properties of the CoP trajectories reflects: (i) the adaptive nature of postural control solutions to the external changes of the support surface, and (ii) the changing within-trial variability of CoP motion. Collectively, the adaptive mixture of deterministic and stochastic variability present in the signals supports the notion of stable and flexible postural solutions as a function of angle of postural support.

Consistent with the CoP findings, the VTC dynamics showed similar directional changes between the different slopes of the support surface. It has been shown that VTC is more sensitive in revealing postural modulations than traditional CoP variability measures due to VTC capturing a higher order dimension (i.e. velocity and acceleration) of control relative to a stability boundary [19]. Here, the results revealed deterministic and stochastic structures within VTC trajectories that were also dependent on the slope of the support surface. A methodological limitation of our approach to creating a slope is that for our model the wedged structure is viewed as a part of the subject and not the force-plate, though we did not find any data trend that reflected a problem.

The platform slope manipulations induced asymmetrical changes of the organization of the musculoskeletal properties pertinent to postural control. Given the simple hinge mechanisms of the ankle joint, where the range of motion is typically between +25° (dorsiflexion) to - 45° (plantarflexion) [22], we were able to capture a range of slopes that approached the anatomical limits of the ankle motion range. Also, during quiet standing an ankle strategy is typically used to maintain postural stability [5] and, therefore dorsi- and plantar-flexion deviations from the flat surface alter the proprioceptive information arising the ankle joint, sensory feedback from muscle length change in the plantarflexion/dorsiflexion position of the postural stance [23]. Nonetheless, postural stability was maintained presumably in part due to the multiple feedback control loops as well as feedforward signals that

Table 2
CoP and VTC recurrence dynamics parameters for trial 1 and trial 2 across sloped platform conditions.

Recurrence Parameter	%REC				%DET				ENT				%LAM			
Regression Values	adjusted R^2		RMSE		adjusted R^2		RMSE		adjusted R^2		RMSE		adjusted R^2		RMSE	
Trial Number	1	2	1	2	1	2	1	2	1	2	1	2	1	2	1	2
CoP_{ML}	0.88	0.90	0.74	0.62	0.95	0.89	0.09	0.39	0.86	0.81	0.28	0.12	0.95	0.88	0.22	0.56
CoP_{AP}	0.76	0.81	0.57	0.58	0.51	0.69	0.23	0.29	0.96	0.85	0.09	0.05	0.93	0.92	0.13	0.37
VTC	0.94	0.91	0.30	0.29	0.90	0.88	0.13	0.14	0.67	0.12	0.71	0.09	0.81	0.87	0.28	0.21

RMSE: Root Mean Square Error. **CoP_{ML}** (medio-lateral) is along x direction, and **CoP_{AP}** (anterior-posterior) is along y direction of force-plate.

operate over various time scales and were adaptable to both internal and external perturbation [1,12].

The modulation of the recurrent dynamics for both CoP and VTC trajectories may be a mechanism to stabilize posture with increasing constraints without a detrimental loss of information. The sloped surfaces induced a more rigid control strategy (specific variable findings) compared to the flat surface for both signals. This rigidity potential relates to a safety mechanism designed to reduce the active degrees of freedom and to maintain the center-of-mass within the stability boundary. Other postural manipulations, such as foot orientation [3] and visual input [21], have also produced rigid postural control strategies.

Secondly, the trajectories of both CoP and VTC showed decreased *%LAM* in the sloped surfaces independent of postural stability on slope angles. The *%LAM* quantifies the vertical line structure of the recurrence plot and indicates the duration of specific states of the system. The finding of fewer laminar states for the sloped surfaces suggests that the postural control system may be using these changing states to explore the reduced stability boundaries of the sloped surfaces. This is consistent with the notion that small-scale postural variability reflects a search strategy of the perceptual-motor workspace to facilitate the maintenance of upright standing [24,25]. The manipulation of the slope of the surface of support in real time would provide a more direct examination of the adaptive potential of dorsiflexion and plantarflexion in postural control.

Overall, the experimental findings revealed that the dynamics of the CoP within the functional stability boundary (VTC) reflected an adaptive mix of dispersion and regularity through asymmetrical modulation of deterministic and stochastic properties to produce stable, yet flexible postural solutions. The recurrent dynamics of VTC operate on a more fine grained dimensional scale than that of CoP and may relate to its enhanced sensitivity to determining stability [26] but showed a similar pattern of change over the reduced stability region of the sloped conditions as the CoP. We speculate that these outcome measures in the context of the functional stability region may serve as a biomarker for the onset of postural instability in pathologies or populations with chronic ankle instability.

Declaration of interest

Authors have no disclosers to make

Authors contributions

Data Collection: ADM; Conceptualization: ADM ACK KMN; Analysis: ADM ACK; Supervision: KMN, Validation: KMN; Writing: ADM ACK KMN

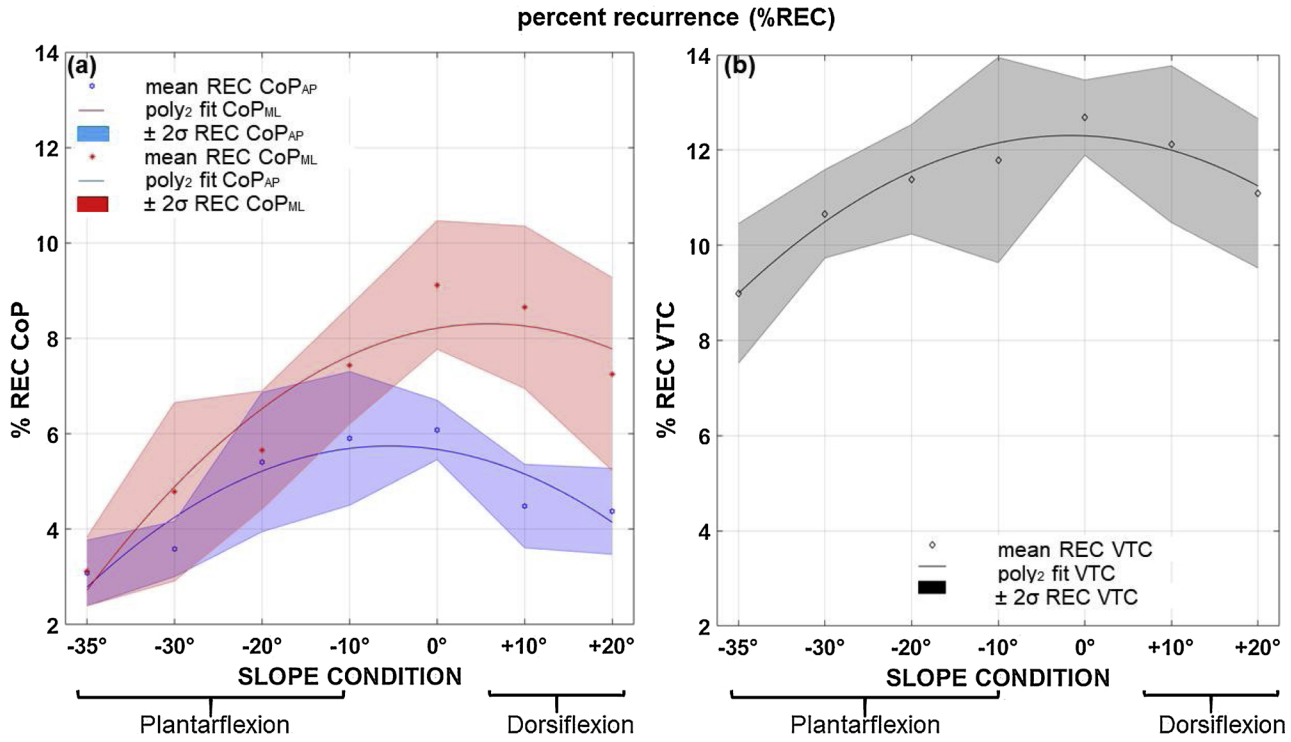

Fig. 2. Mean ± SD for percent recurrence (%REC) of (a) CoP-ML & CoP-AP and (b) VTC for Trial 1.

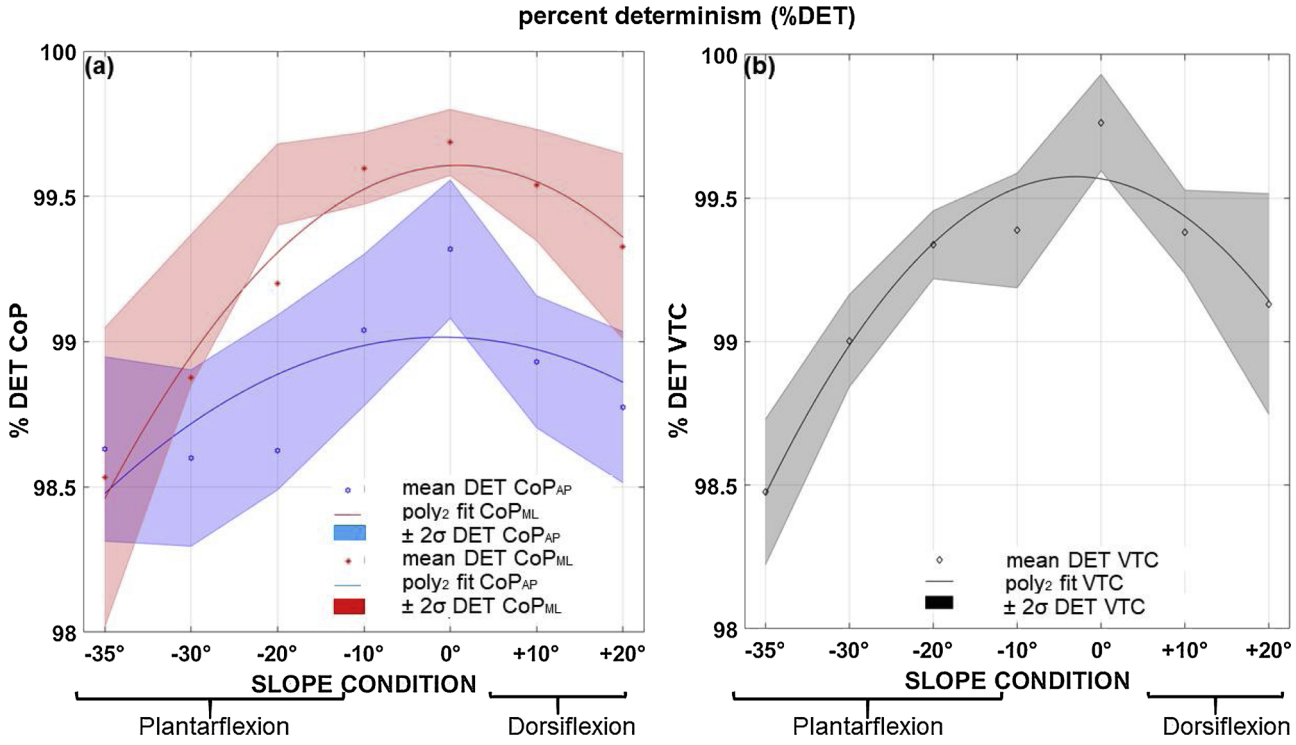

Fig. 3. Mean ± SD for percent determinism (%DET) of (a) CoP-ML & CoP-AP and (b) VTC for Trial 1.

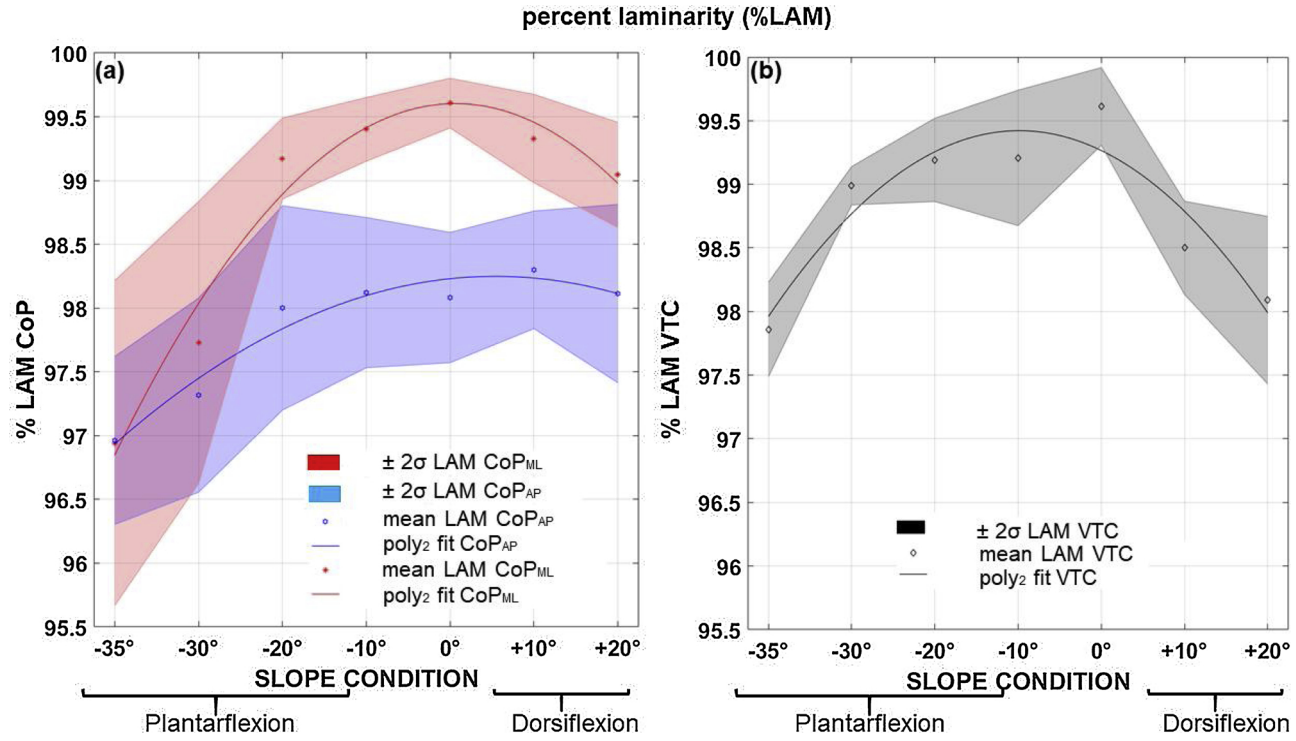

Fig. 4. Mean ± SD for percent laminarity (%LAM) of (a) CoP-ML & CoP-AP and (b) VTC for Trial 1.

Appendix A

Virtual Time-To-Contact

The general algorithm to calculate VTC and determine the functional stability boundary was primarily replicated from Slobounov's work [17]. To calculate the VTC value for each instantaneous measured position of the CoP (object in our case), the real time was stopped at a current moment (τ_i) and the virtual motion of the object with constant acceleration was simulated. The resultant force as well as acceleration $a(\tau_i)$ were constant while

the object was moving along its virtual trajectory from the current initial position $r(\tau_i)$ with instantaneous initial velocity $v(\tau_i)$ until it would collide with the stability boundary. Here, (x_c, y_c) denotes the point on the stability boundary where the virtual trajectory intersects it for the first time. If the end points of the corresponding boundary line segment are (x_1, y_1) and (x_2, y_2) the slope (s) of the line connecting the two points is

$$s = (y_2 - y_1)/(x_2 - x_1)$$

Assuming constant slope in the differential segment between (x_1, y_1) and (x_2, y_2), the slope can subsequently also be computed as

$$s = (y_c - y_1)/(x_c - x_1)$$

Assuming a point massless model for the CoP with constant acceleration, the point of virtual time-to-contact can be written as

$$x_c(\tau) = r_x + v_x.\,\tau + a_x.\,{\tau^2}/{2}$$

$$y_c(\tau) = r_y + v_y.\,\tau + a_y.\,{\tau^2}/{2}$$

Substituting x_c and y_c from $x_c(\tau) = r_x + v_x.\,\tau + a_x.\,{\tau^2}/{2}$ and $y_c(\tau) = r_y + v_y.\,\tau + a_y.\,{\tau^2}/{2}$ in $s = (y_c - y_1)/(x_c - x_1)$, and equating it to $s = (y_2 - y_1)/(x_2 - x_1)$, gives a quadratic equation in τ. VTC (τ) is the lowest positive solution of this quadratic equation.

Appendix B

Recurrence Parameter Selection

The CoP sway along both x (ML) and y (AP) directions, and VTC were analyzed using recurrence measures. Standard approaches, as outlined by [12,27] were used to determine the input parameters of the recurrence analysis. In brief, the time-series pertaining to CoP and VTC were reconstructed phase space trajectories using the standard time delay method. We used the false nearest neighbor method and average mutual information approaches to determine the appropriate embedding dimension (m) and time-delay (τ), respectively. Thereafter, a sphere with a *radius* of 25% of the mean distance separating points in reconstructed phase space was used to ensure that the percent recurrence remained below 5%. These input parameters (CoP, $m = 5$; VTC, $m = 8$ and $\tau = 10$) were used to create recurrence plots for each signal independently (Fig. 1).

References

[1] L. Nashner, G. McCollum, The organization of human postural movements: a formal basis and experimental synthesis, Behav. Brain Sci. 8 (1985) 135–150.
[2] F.B. Horak, Postural orientation and equilibrium: what do we need to know about neural control of balance to prevent falls? Age Ageing 35 (2006) ii7–ii11.
[3] A.C. King, Z. Wang, K.M. Newell, Asymmetry of recurrent dynamics as a function of postural stance, Exp. Brain Res. 220 (2012) 239–250.
[4] A. Dutt-Mazumder, S.M. Slobounov, J.H. Challis, K.M. Newell, Postural stability margins as a function of support surface slopes, PLoS One 11 (2016) e0164913.
[5] D. Winter, Biomechanics and Motor Control of Human Movement, John Wiley & Sons, Ltd, New Jersey, 2009.
[6] V.M. Zatsiorsky, M. Duarte, Instant equilibrium point and its migration in standing tasks: rambling and trembling components of the stabilogram, Motor Control 3 (1999) 28–38.
[7] B.A. McClenaghan, H.G. Williams, J. Dickerson, M. Dowda, L. Thombs, P. Eleazer, Spectral characteristics of aging postural control, Gait Posture 4 (1996) 112–121.
[8] N. Stergiou, L.M. Decker, Human movement variability, nonlinear dynamics, and pathology: Is there a connection? Hum. Mov. Sci. 30 (2011) 869–888.
[9] J.P. Carroll, W. Freedman, Nonstationary properties of postural sway, J. Biomech. 26 (1993) 409–416.
[10] M. Duarte, V.M. Zatsiorsky, Long-range correlations in human standing, Phys. Lett. A 283 (2001) 124–128.
[11] N. Marwan, M. Thiel, N. Nowaczyk, Cross recurrence plot based synchronization of time series, nonlinear process, Geophys. 9 (2002) 325–331.
[12] M. Riley, R. Balasubramaniam, M. Turvey, Recurrence quantification analysis of postural fluctuations, Gait Posture 9 (1999) 65–78.
[13] C.L. Webber Jr, N. Marwan, Theory and best practices, Recurrence Quantification Analysis, 1st ed., Springer International Publishing, 2015.
[14] K. Shockley, M. Butwill, J.P. Zbilut, C.L. Webber, Cross recurrence quantification of coupled oscillators, Phys. Lett. A 305 (2002) 59–69.
[15] S. Clark, M.A. Riley, Multisensory information for postural control: sway-referencing gain shapes center of pressure variability and temporal dynamics, Exp. Brain Res. 176 (2007) 299–310.
[16] N.B. Alexander, Postural control in older adults, J. Am. Geriatr. Soc. 42 (1994) 93–108.
[17] S.M. Slobounov, E.S. Slobounova, K.M. Newell, Virtual time-to-collision and human postural control, J. Mot. Behav. 29 (1997) 263–281.
[18] S.M. Slobounov, P.S. Haibach, K.M. Newell, Aging-related temporal constraints to stability and instability in postural control, Eur. Rev. Aging Phys. Act. 3 (2006) 55–62.
[19] P.S. Haibach, S.M. Slobounov, E.S. Slobounova, K.M. Newell, Virtual time-to-contact of postural stability boundaries as a function of support surface compliance, Exp. Brain Res. 177 (2007) 471–482.
[20] C.K. Rhea, T.A. Silver, S.L. Hong, J.H. Ryu, B.E. Studenka, C.M.L. Hughes, J.M. Haddad, Noise and complexity in human postural control: Interpreting the different estimations of entropy, PLoS One 6 (2011) e17696.
[21] J.M. Kinsella-Shaw, S.J. Harrison, C. Colon-Semenza, M.T. Turvey, Effects of visual environment on quiet standing by young and old adults, J. Mot. Behav. 38 (2006) 251–.
[22] C.L. Brockett, G.J. Chapman, Biomechanics of the ankle, Orthop. Trauma 30 (2016) 232–238.
[23] A. Dutt-Mazumder, R. Segal, L. Davis, A. Thompson, J. Dean, Morphological and reflex properties of soleus during ankle flexion, in: soc, Neurosci. Meet., Washington, DC (2017).
[24] G. Riccio, Information in movement variability about the qualitative dynamics of posture and orientation, in: K. Newell, D. Corcos (Eds.), Var. Mot. Control, Human Kinetics, Champaign, IL, 1993, pp. 317–358.
[25] M.A. Riley, M.T. Turvey, Variability and determinism in motor behavior, J. Mot. Behav. 34 (2002) 99–125.
[26] A. Dutt-Mazumder, T. Rand, M. Mukherjee, K.M. Newell, Scaling oscillatory platform frequency reveals recurrence of intermittent postural attractor states, Sci. Rep. (2018).
[27] C. Webber, J. Zbilut, Recurrence quantifications: feature extractions from recurrence plots, Int. J. Bifurcat. Chaos 17 (2007) 3467–3475.